Lei, S-F., Hamernik, R.P. (1995). Wavelet Transform and Frequency Domain Kurtosis: Application to Assessment of Hearing Hazard from Noise Exposure. Proceedings *IEEE Applications of Signal Processing to Audio and Acoustics.* pp.1.4.1-3, New Paltz, NY, IEEE publishers, NJ.

WAVELET TRANSFORM AND FREQUENCY DOMAIN KURTOSIS: APPLICATION TO ASSESSMENT OF HEARING HAZARD FROM NOISE EXPOSURE

Sheau-Fang Lei and Roger P. Hamernik

Auditory Research Laboratory
State University of New York
Plattsburgh, NY 12901

ABSTRACT

Research on the effects of noise on the auditory system has shown that the frequency domain kurtosis (FDK) statistic could be a useful metric in quantifying a noise environment for hearing conservation purposes. Joint time-frequency analytical methods used in signal processing may be of use in the extraction of such information from an exposure environment characterized by nonstationary signals. This paper shows that the FDK metric can be efficiently computed by applying the wavelet transform to the analysis of an acoustic signal.

1. INTRODUCTION

At present the evaluation of a noise exposure for the purpose of hearing conservation practice relies primarily upon a measure of the frequency weighted average energy of an exposure. Temporal variables of the noise waveform are completely neglected. Recent studies [1, 2] however have shown that an understanding of the temporal structure of a noise is critical to predicting the hearing trauma. Such results imply that the conventional metrics used to characterize noise exposure such as sound pressure level (SPL) and time-averaged spectrum are not adequate for estimating the hazard to hearing from many types of industrial/military noise environments.

In many industrial work environments, the waveform of an acoustic noise typically consists of randomly occurring impulses or other transient components superimposed on a time-varying continuous background Gaussian component. This type of noise would be more accurately described as a non-Gaussian, and nonstationary stochastic signal. Such signals may have an SPL and spectrum which is similar to that of a Gaussian noise but very different temporal characteristics that may affect the accumulation of hearing loss. Animal model experiments have demonstrated that this is indeed the case, i.e., noises having the same energy and spectra but differing considerably in their temporal structures produce very different hearing loss and cochlear pathology, which is distributed differently across audiometric test frequencies. Using these experimental results as a background, Lei et al. [1] have shown that the frequency-domain kurtosis (FDK) in conjunction with an energy metric is useful in quantifying a signal's potential for producing hearing loss. FDK extracts the kurtosis statistic from the temporal distribution of the amplitude fluctuations as a function of frequency. Thus the FDK metric provides an indication of the regions of the frequency spectrum in which the signal undergoes nonstationary fluctuations and the extent of these fluctuations relative to Gaussian conditions. Analytical methods which can transform a nonstationary signal into a joint time-frequency representation are preferable if the FDK metric is to be efficiently obtained. The wavelet transform has been developed as a practical tool for the analysis of nonstationary signals. In this paper, synthesized signals having some basic features in common with acoustic noise environments are analyzed using the wavelet transform algorithm on a logarithmic frequency scale. Such a scale shares features in common with the cochlear transduction process. The FDK metric is then computed from the results of the wavelet transform.

2. ANALYTICAL APPROACH

2.1 Wavelet transform

The wavelet transform decomposes a time-varying signal into a time frequency function in which signal events are localized in both time and frequency. The wavelet transform bears a resemblance to the short-time Fourier transform (STFT) in signal processing. However, the wavelet transform has the advantage that the signal spectrum can be decomposed into nonoverlapping frequency bands on a logarithmic scale. This decomposition can be accomplished by transforming the signal into a set of orthogonal bases which are called "wavelets". All wavelets are scaled and translated versions of one generating function, $\phi(x)$, constructed from the solution to a set of two recursive difference equations:

$$\phi(x) = \sum_{k=0}^{M-1} c_k \, \phi(2x-k)$$

dilation equation (M is the finite number of coefficients)

$$\psi(x) = \sum_{k} (-1)^k c_{1-k} \, \phi(2x-k)$$

wavelet equation

Daubechies [3] obtained the solution to $\phi(x)$ for a given M and the properties of the related coefficients c_k and thus the solution for $\psi(x)$. The Mallat's pyramid algorithm (or tree algorithm) [4] is a computationally efficient method of implementing the wavelet transform. This algorithm enables the wavelet transform to be computed in the form of a discrete wavelet transform (DWT) without finding $\phi(x)$ and $\psi(x)$ explicitly. The pyramid algorithm operates on a finite set of input data whose length is an integer power of two. These data are passed through two convolution functions, each of which generates an output stream that is half the length of the original input by keeping every other sample of the output (i.e., by subsampling by a factor of 2). These convolution functions essentially act as filters. One half of the output is produced by lowpass filtering through a filter whose impulse response is equivalent to the coefficients c_k of the dilation equation, and the other half is produced by highpass filtering through a filter whose impulse response is related to the coefficients of the wavelet equation. This algorithm can be considered as a decomposition of the signal of interest into coarse and fine detail components as shown in Figure 1. The output sequence of the

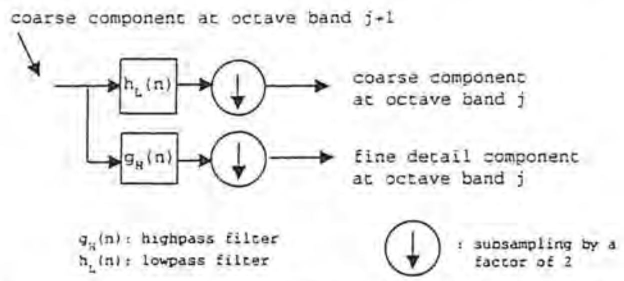

Figure 1. The basic structural unit for implementing Mallat's pyramid algorithm for signal decomposition into coarse and fine detail components.

lowpass filtering contains the coarse components while the highpass filtering produces the fine detail components of the input signal. These two convolutions are iteratively performed on a binary scale (e.g. logarithmic or octave band frequency scale). Due to the orthogonality and invertibility of the DWT, the fine detail components in each scale can be used to reconstruct the contributed sample of the total signal in that scale by performing the inverse DWT (IDWT) with the same pyramid algorithm. The superposition of all the contributed samples for each scale recovers the original input signal since the DWT is a linear operator. The reconstructed components for each scale represent the filtered output sequences of a group of filter banks whose bandwidths are set to a binary scale.

2.2 Frequency domain kurtosis

Kurtosis is defined as the ratio of the fourth-order central moment to the squared second-order central moment of the sample distribution. The kurtosis of a non-Gaussian stochastic signal can be used to measure or estimate the "peakedness" of the amplitude distribution. Erdreich [5] suggested that the kurtosis of the amplitude distribution could be used as a metric to evaluate the effects of the temporal peak distribution properties of a noise exposure on hearing. Dwyer [6] used the frequency domain kurtosis (FDK) to detect the presence of randomly occurring non Gaussian components in a signal when the frequency spectrum of that signal varied from moment to moment. Dwyer's algorithm uses the STFT operating on linear frequency scale to obtain FDK. The FDK results computed using Dwyer's algorithm proved difficult to relate to the audiometric and histological effects that resulted from the exposures of experimental animals to various non-Gaussian noises. Part of the reason for this is that the micromechanics of the cochlear transduction processes operate in a manner that maps frequency information logarithmically over the basilar membrane as a continuous function of time. This paper presents a modified FDK algorithm computed on a logarithmic frequency scale rather than linear scale using the wavelet transform.

3. PRELIMINARY RESULTS

Two simulated acoustic waveforms, one Gaussian, the other an impulsive transient, are shown in Figure 2. These two waveforms,

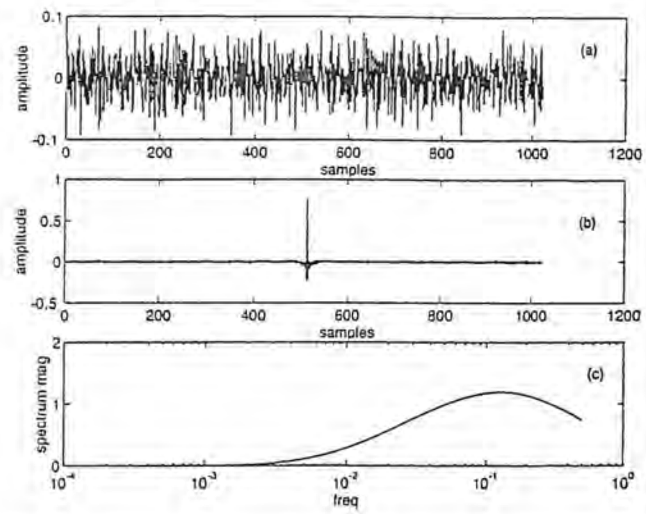

Figure 2. The acoustic waveforms and frequency spectra of the two test signals. (a) Gaussian waveform, (b) impulsive waveform, (c) frequency spectra of the Gaussian and impulsive waveforms.

generated using the algorithm described by Hsueh and Hamernik [7], have identical spectra [Figure 2(c)]. These two waveforms were processed using the DWT with Mallat's pyramid algorithm. The Daubechies approach with 18 wavelet coefficients (i.e., M=18) was used for the impulse response of the convolution filters in the pyramid algorithm. The output sequence for each octave band was reconstructed from the fine detail component in each band using the inverse DWT. The output sequence of three successive octave bands for both the Gaussian noise and impulsive noise is shown in Figures 3(a) and 4(a) respectively. The frequency spectrum of each corre-

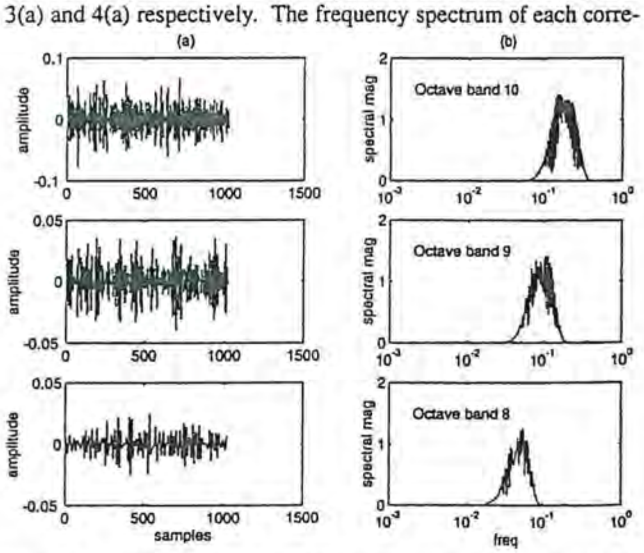

Figure 3. The output sequences from three successive octavebands of the Gaussian waveform reconstructed using the IDWT (implemented by Mallat's pyramid algorithm). (a) the reconstructed waveforms. (b) the corresponding frequency spectra.

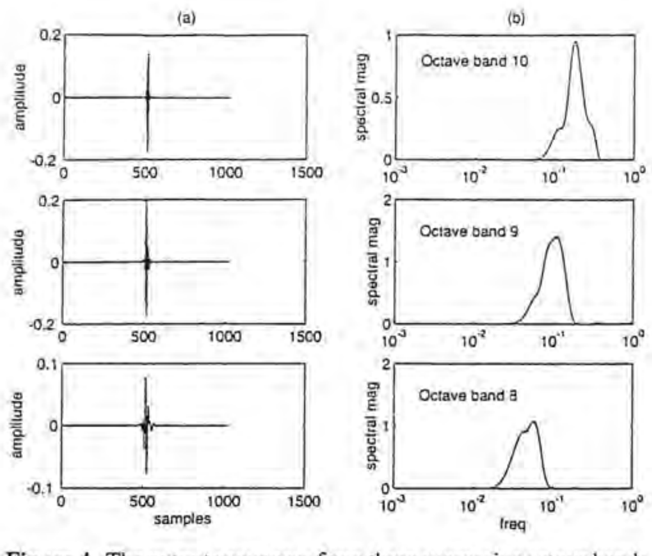

Figure 4. The output sequences from three successive octave bands of the impulsive waveform reconstructed using the IDWT (implemented by Mallat's pyramid algorithm). (a) the reconstructed waveforms. 4(b) the corresponding frequency spectra.

sponding sequence is plotted in Figures 3(b) and 4(b). These frequency spectra confirm that the three output sequences are of three different octave bands. The temporal distinctions between the Gaussian noise and the impulsive noise can be seen in the output sequences of the corresponding octave bands. The occurrence of the impulse temporal waveform is preserved in each sequence after application of the DWT while this information is lost in the conventional frequency spectrum. The FDK metric can now be computed from the output sequence for each corresponding octave band. The FDK results for both of the simulated noises is shown in Figure 5. The FDK values for the Gaussian noise are around 3 for all octave bands since decomposition of the Gaussian noise yields a Gaussian signal in each octave band. The FDK values for the impulsive noise are higher than those of Gaussian noise because the output sequence for every octave band has an impulsive component. Thus the differences in the temporal information between these two noises are preserved using the wavelet transform and are reflected in the estimates of FDK.

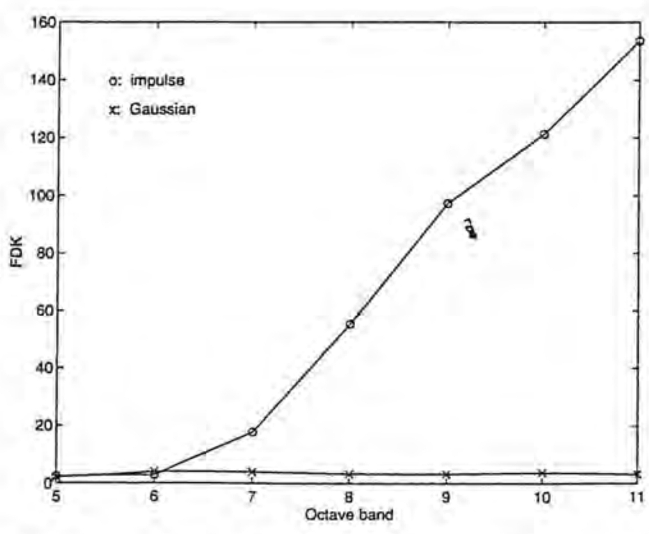

Figure 5. FDK values for adjacent octave bands of the Gaussian and impulsive noises.

REFERENCES

1. Lei, S.-F., Ahroon, W.A., and Hamernik, R.P. "The application of frequency and time domain kurtosis to the assessment of hazardous noise exposures" J. Acoust. Soc. Am. Vol. 96, pp. 1435-1444, 1994.

2. Dunn, D.E., Davis, R.R., Merry, C.J., and Franks, J.R. "Hearing loss in the chinchilla from impact and continuous noise exposure," J. Acoust. Soc. Am. Vol. 90, pp. 1979-1985, 1991.

3. Daubechies, I. "Orthonormal bases of compactly supported wavelets" Comm. Pure Applied Mathematics, Vol. 41, pp. 909-996, 1988.

4. Mallat, S.G. "A theory of multiresolution signal decomposition: the wavelet representation," IEEE Trans. Pattern Anal. Machine Intell., Vol. 11, pp. 674-693, 1989.

5. Erdreich, J. "A distribution based definition of impulse noise," J. Acoust. Soc. Am., Vol.79, pp. 990-998, 1986

6. Dwyer, R.F. "Use of the kurtosis statistic in the frequency domain as an aid in detecting random signals," IEEE J. Oceanic Eng., Vol.OE-9, pp. 85-92, 1984.

7. Hsueh. K.D., Hamernik, R.P. "A generalized approach to random noise synthesis: Theory and computer simulation," J. Acoust. Soc. Am., Vol. 87, pp. 1207-1217, 1990.

ACKNOWLEDGEMENT

We gratefully acknowledge the support of the National Institute for Occupational Safety and Health (grant numbers K01-OH00139 and R01-OH02317).